Supplementary figure 1.

Cell characterization: **a.** BM-MSCs were cultured up to maximum 9 cell passages and cell morphology was assessed at each passage using a phase contrast Zeiss Axiovert 135 microscope (100µm scale bar in the 10x magnification photo; 50µm scale bar in the 32x magnification photo). **b-c.** Mesenchymal differentiation potential. BM-MSCs at the 5th passage were induced to differentiate into adipocytes by defined medium [11]. Adipogenesis was assessed with Oil red O staining on untreated (**b.**) and treated (**c.**) cells (20x). **d.** Immunophenotype. BM-MSCs at passage 5 were harvested and stained for specific cell surface antigens. At flow-cytometric analysis, cells were positive for mesenchymal stem cell markers (CD29, CD44, CD73, CD90) and negative for endothelial markers (CD31). The control isotype is indicated in light grey. **e.** AFS cell lines were cultured on non-tissue culture petri dishes as previously reported . **f.** Immunophenotype. At flow-cytometry and immunofluorescence analyses, AFS cells were negative for hematopoietic (CD45) and positive for mesenchymal (CD73, NFGr, CD105, Vimentin) markers. **h.** Phase contrast image of the three different clones (E8, E9, E11) used in the experiments showed a normal karyotype (scale bar= 20µm, 40x magnification). **i.** A line of committed cells, i.e. rat skeletal muscle myoblasts, were used as a supplementary negative control vs. AFS cells in rat NEC. Cell morphology was assessed using a phase contrast Zeiss Axiovert 135 microscope (100µm scale bar in the 10x magnification photo; 50µm scale bar in the 32x magnification photo).

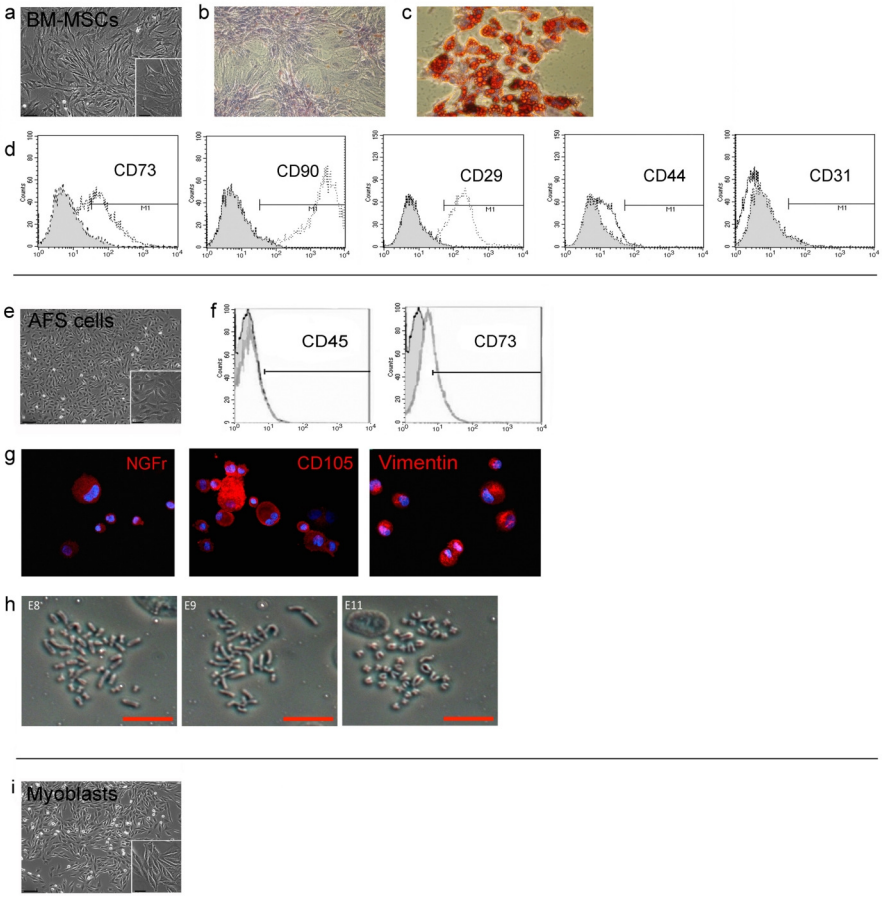
a
BM-MSCs
b
c
d
CD73
CD90
CD29
CD44
CD31
e
AFS cells
f
CD45
CD73
g
NGFr
CD105
Vimentin
h
E8
E9
E11
i
Myoblasts

Supplementary figure 2.

NEC rats injected intraperitoneally (i.p.) with BM-MSCs (n=26; Fig. **supplementary 1**) at 24 and 48 hours of life did not show improved survival compared with animals injected with phosphate buffered saline (PBS; n=30) (Fig. 1a). Age-matched breastfed rats (BF=12) not subjected to NEC induction and used as controls, had 92% survival ($p<0.0001$) (**Fig. supplementary 2a**). Considering this lack of effect, NEC rats were injected with AFS cells, BM-MSCs, myoblasts (n=21, as a committed negative control) or PBS (n=43) and compared with BF rats (**Fig. 1b and supplementary 2b**).

a

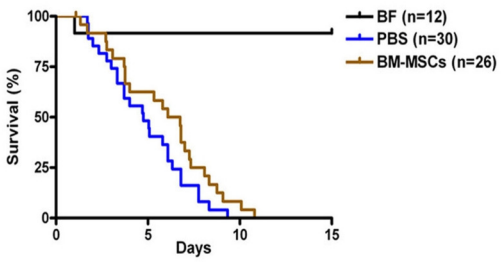
BF (n=12)
PBS (n=30)
BM-MSCs (n=26)
Survival (%)
Days
0
25
50
75
100
0
5
10
15

b

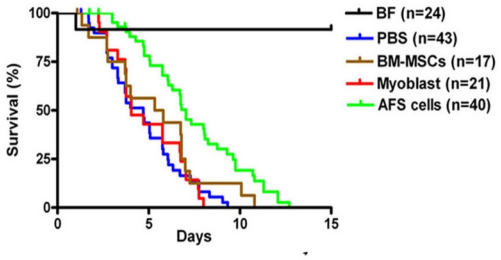
BF (n=24)
PBS (n=43)
BM-MSCs (n=17)
Myoblast (n=21)
AFS cells (n=40)
Survival (%)
Days
0
25
50
75
100
0
5
10
15

c

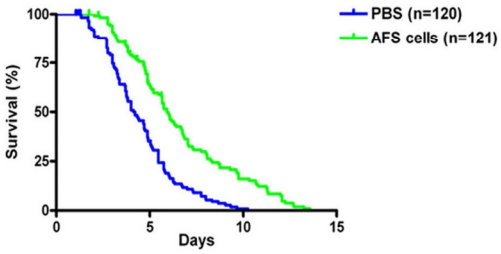
PBS (n=120)
AFS cells (n=121)
Survival (%)
Days
0
25
50
75
100
0
5
10
15

Supplementary figure 3.

Peritoneal fluid accumulation, (assessed using MRI imaging as voxels with T2>160ms) was significantly greater in the NEC rats injected with PBS, than those treated with AFS or the BF rats (**Supplementary Fig. 3a**). In addition, using high-resolution µMRI after gadolinium fixation [23], PBS pups, similarly to human infants with NEC, but not AFS or BF animals, displayed dilated bowel loops, with significantly thinned gut walls (**Supplementary Fig. 3b**).

a

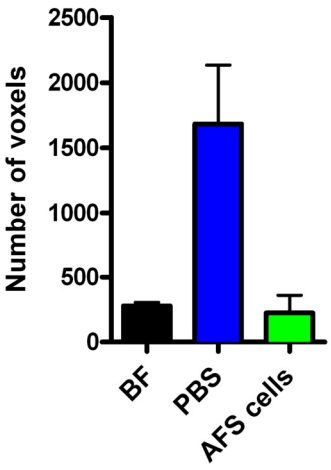
Number of voxels
2500
2000
1500
1000
500
0
BF
PBS
AFS cells

b

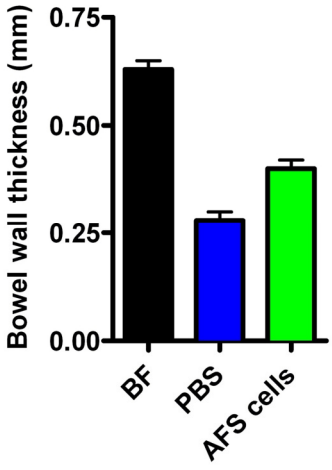
Bowel wall thickness (mm)
0.75
0.50
0.25
0.00
BF
PBS
AFS cells

Supplementary figure 4.

a. NEC rats received an i.p. injection of either PBS, AFS cells, CM or α-MEM at 24 and 48 hours of life and were followed until natural death occurred. **b**. At 7 days of life, NEC rats treated with CM had a similar survival rate of those treated with AFS cells (p=n.s.), but had a higher survival than those treated with PBS ($p< 0.01$) or with α-MEM ($p< 0.001$). **c.** The overall survival study confirmed that CM injected rats had a significant longer survival than rats injected with PBS ($p< 0.01$) or with α-MEM ($p<0.0001$). Similarly AFS cells injected rats had a significant longer survival than rats injected with PBS ($p< 0.001$) or with α-MEM ($p<0.0001$). No differences were noted between AFS cell group and CM group (p=n.s.).

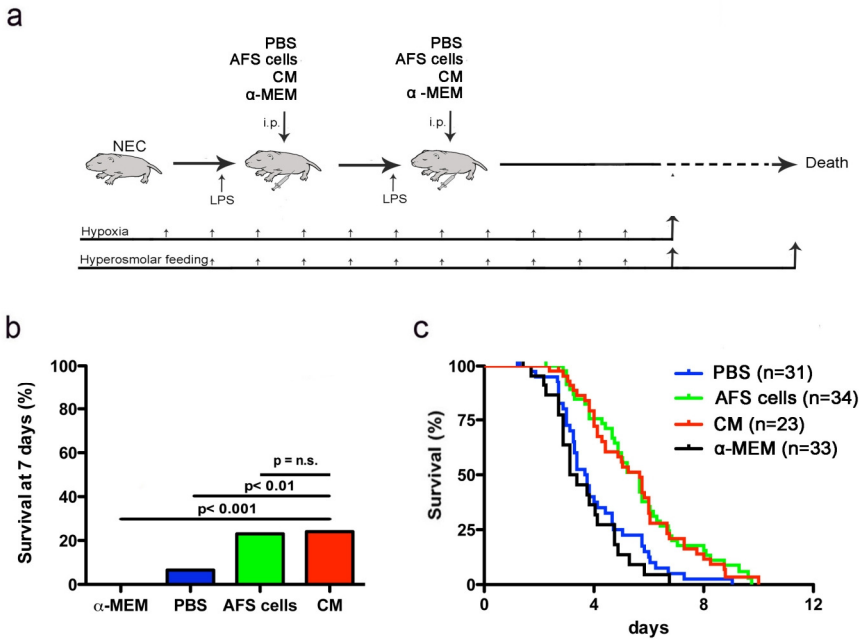
a
PBS
AFS cells
CM
α-MEM
i.p.
PBS
AFS cells
CM
α -MEM
i.p.
NEC
LPS
LPS
Death
Hypoxia
Hyperosmolar feeding
b
Survival at 7 days (%)
100
80
60
40
20
0
p = n.s.
p< 0.01
p< 0.001
α-MEM
PBS
AFS cells
CM
c
Survival (%)
100
75
50
25
0
0
4
8
12
days
PBS (n=31)
AFS cells (n=34)
CM (n=23)
α-MEM (n=33)

Supplementary figure 5.

This cartoon explains the beneficial action mechanism of AFS cells on damaged gut epithelium: (I) i.p. injected AFS cells activate resident COX-2+ cells via a paracrine effect; (II) as a result, COX-2+ cells migrate from the villus axis down to the crypt, where they stimulate resident stem cells to repopulate the sloughed epithelium.

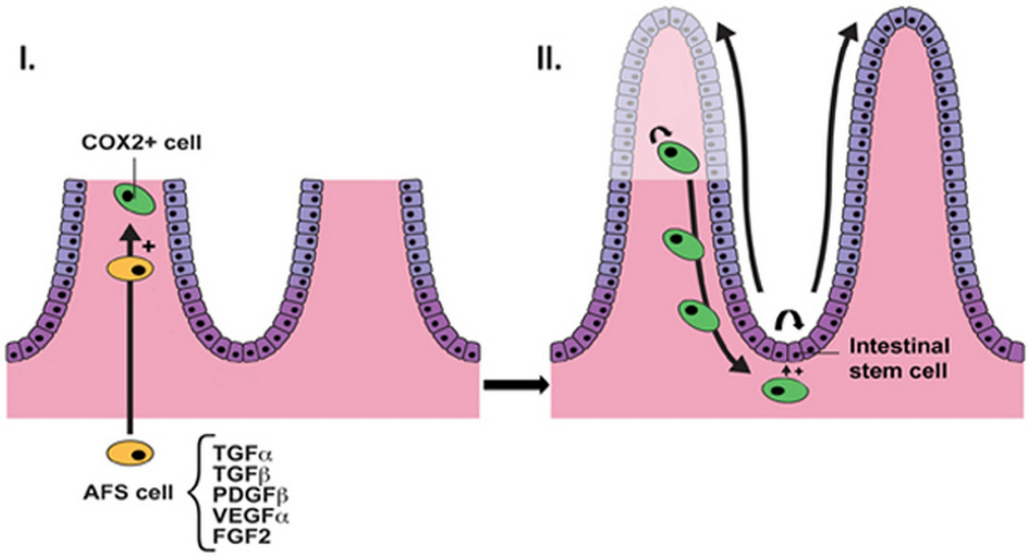

Supplementary methods

Magnetic Resonance Imaging. Images were acquired at two stages. In stage one, pups were imaged immediately after sacrifice (AFS[n=3], PBS [n=3], BF [n=2]). Multi-slice spin-echo axial images were acquired at echo times of 15, 20, 30 and 45ms to generate T2 maps for visualisation of abdominal fluid. Other parameters were: no of slices = 40; in plane matrix size = 128 × 128; field of view = 19.2mm × 19.2mm; slice thickness = 0.5mm; slice separation = 0mm; repetition time = 3.5s. T2 maps were generated by fitting a mono-exponential decay model to the images acquired at increasing echo times. In stage 2, 1 pup from each group was imaged using μMRI methods [23]. Directly after stage 1 imaging, pups were immersed in 4% formaldehyde solution (from paraformaldehyde), doped with 8mM gadolinium-diethylenetriaminepentaacetic acid (Gd-DTPA, [Magnevist], Bayer–Schering, Newbury, UK) and placed on a rotator for 3 weeks. Pups (1 from each group) were scanned using a 3D gradient echo sequence. Parameters were: matrix size 512×512×512; imaging volume = 27 × 27 × 27mm; echo time =6ms; repetition time = 20ms; flip angle =60^{o}; number of averages = 8; 10 dummy scans. From the high resolution images, bowel wall thicknesses were measured in 5 axial slices in the same plane using the following anatomical landmarks: the top, bottom and midpoint of the right kidney, and the midpoint and bottom of the left kidney. Within these slices, only small bowel sections running perpendicular to the axial slice were considered to minimise partial volume effects. The thicknesses of bowel walls were evaluated by measuring the shortest distance between the inner diameter to the outer diameter at 4 points:

the most dorsal, ventral, lateral (sinister and dexter). The extent of fluid accumulation outside the bowels was estimated by counting the number of voxels with a T2 greater than 160ms in the same 5 slices. Voxels with a T2> 160ms within the bowel, bladder and spinal cord and kidney were excluded by manual segmentation based on visual inspection of the images. The threshold of 160ms was chosen based on the lower limit of the 95% confidence interval of the estimated T2 values within a region of fluid in the abdomen. A Student's T-test was used to test for possible differences between the wall thickness measurements as well as between the T2 voxel counts (see **Fig. supplementary 3a and b**).

Supplementary videos. Segment of rat intestine was immersed in oxygenated Krebs solution and maintained at constant length. A video camera linked to a computer recorded intestinal wall movement under isometric conditions. Gut movements of NEC rats (**video1**) are compared to gut derived from AFS cell treated NEC rats (**video 2**).